

# Northumbria Research Link

Citation: Corradi, Marco, Speranzini, Emanuela and Bisciotti, Giordano (2020) Out-of-plane reinforcement of masonry walls using joint-embedded steel cables. Bulletin of Earthquake Engineering. ISSN 1570-761X (In Press)

Published by: Springer

URL: <http://doi.org/10.1007/s10518-020-00875-3> <<http://doi.org/10.1007/s10518-020-00875-3>>

This version was downloaded from Northumbria Research Link: <http://nrl.northumbria.ac.uk/43224/>

Northumbria University has developed Northumbria Research Link (NRL) to enable users to access the University's research output. Copyright © and moral rights for items on NRL are retained by the individual author(s) and/or other copyright owners. Single copies of full items can be reproduced, displayed or performed, and given to third parties in any format or medium for personal research or study, educational, or not-for-profit purposes without prior permission or charge, provided the authors, title and full bibliographic details are given, as well as a hyperlink and/or URL to the original metadata page. The content must not be changed in any way. Full items must not be sold commercially in any format or medium without formal permission of the copyright holder. The full policy is available online: <http://nrl.northumbria.ac.uk/policies.html>

This document may differ from the final, published version of the research and has been made available online in accordance with publisher policies. To read and/or cite from the published version of the research, please visit the publisher's website (a subscription may be required.)



**Northumbria  
University**  
NEWCASTLE



**UniversityLibrary**



# Out-of-plane reinforcement of masonry walls using joint-embedded steel cables

Marco Corradi<sup>1,2</sup> · Emanuela Speranzini<sup>2</sup> · Giordano Bisciotti<sup>3</sup>

Received: 19 February 2020 / Accepted: 19 May 2020  
© The Author(s) 2020

## Abstract

The out-of-plane mechanism (rocking) of walls often causes fatalities and collapses of historic buildings during earthquakes. This paper addresses the problem of assessing the seismic resistance of walls subjected to out-of-plane bending, before and after reinforcement. A new retrofitting method, consisting in the use of high-strength steel cables fully embedded in the mortar bed joints was studied. An experimental investigation using full-scale brickwork specimens was therefore conducted in an attempt to assess the walls' structural response when these are subject to out-of-plane loads. Test results demonstrated that it is possible to increase the out-of-plane capacity with the proposed method. A simplified macro-element procedure is also presented along with recommendations for the calculation of the walls' capacity before and after the application of the steel cable reinforcement. Predictions of the magnitude of horizontal force required to cause out-of-plane failure using the proposed procedure and quasi-static analysis procedures are compared with the results of laboratory experiments.

**Keywords** Brickwork masonry · Earthquake engineering · Mechanical testing · Out-of-plane loading · Retrofitting methods

## 1 Introduction

Earthquakes are a serious problem not only for the safety of people, but also for their economic cost. The Italian State Aid for reconstructing or retrofitting damaged buildings in Abruzzo and Emilia regions, after the 2009 and 2012 earthquake, is estimated to be 26 billion euros (Italian Senate 2017). For the 2016 Central Italy earthquake, an initial evaluation of the State Aid needed for repair and reconstruction of the local building stock is about 11 billion euros. As order of magnitude, Italy's entire government budget deficit was 37 billion in 2018.

---

✉ Marco Corradi  
marco.corradi@northumbria.ac.uk

<sup>1</sup> Department of Mechanical and Construction Engineering, Northumbria University, Newcastle upon Tyne NE1 8ST, UK

<sup>2</sup> Department of Engineering, University of Perugia, Via Duranti 93, 06125 Perugia, Italy

<sup>3</sup> Perugia, Italy

Furthermore, it should be considered that the area heavily struck or damaged by the 2016 Central Italy earthquake is inhabited by only about 600,000 persons (0.99% of the Italian population) and it covers an area of 8000 km<sup>2</sup> (2.66% of the country total area) (King 2015). Although not the whole Italian territory is at risk of a destructive earthquake, the cost for retrofitting the Italian masonry building stock would be much higher and unlikely sustainable for the country.

Historic masonry materials, made of solid clay bricks, rubble or squared up stones, are inherently non-resistant to the seismic actions. There are numerous reasons for these retrofits, but one of the main deficiencies is the low capacity of the buildings' wall panels against out-of-plane actions (D'Ayala and Speranza 2003; D'Ayala and Paganoni 2011; Bui et al. 2017). The out-of-plane rocking of load-bearing walls is a main reason for fatalities and serious damage to the architectural heritage during earthquakes (D'Ayala 2014). To prevent this, increased requirements were recently introduced in the Italian Building Code (2018).

Borri and Corradi (2019) noted that previous design codes did not specify clear criteria or limits for the out-of-plane behavior of load-bearing walls. These criteria were progressively introduced in Italy after the 1976 Friuli earthquake. As such, there is a need in many old masonry buildings to enhance the out-of-plane capacity of single structural members or the whole building. The available methods for the design and analysis of the out-of-plane behavior of masonry structures typically involve the equilibrium of masonry macro-elements (de la Llera et al. 2000; Lagomarsino and Resemini 2009; Giresini et al. 2019). More recently, homogenization approaches have been proposed by several researchers (Milani et al. 2006; Wang et al. 2018; Di Nino and Luongo 2019). Both equilibrium-based and homogenization methods have been also adapted to include retrofitting solutions.

Historically, the walls' out-of-plane rocking has been effectively prevented using metal ties or steel-rod wrappings (Fig. 1) (Putrino and D'Ayala 2020). The current focus of research in this area is the use of Fibre Reinforced Polymers (FRP). Many researchers have used FRP strips bonded to the wall faces with epoxy resin (Gilstrap and Dolan 1998; Velazquez-Dimas and Ehsani 2000; Tumialan et al. 2003; Hamed and Rabinovitch 2007) (Fig. 2). Significant capacity increases have been achieved using this technique, however there are two main drawbacks. First of all, in most applications, it is the debonding of the FRP strip from the masonry substrate itself that governs the capacity enhancement. Regardless of the number of strips of FRP used, if the force cannot be transferred between the strips and the masonry, the enhancement can only reach a maximum dictated by the available bond length.

**Fig. 1** An example of a provisional intervention aimed at preventing the out-of-plane rocking of the façade



**Fig. 2** Example of an “innovative” retrofitting solution using FRP unidirectional strip



Steel cables, rods and ties (Modena et al. 2002; Paganoni and D’Ayala 2014; Jurina 2017) (Fig. 3a) and, more recently, FRP strips (Hamed and Rabinovitch 2005; Korany and Drysdale 2006) have been widely used to stabilize historic masonry towers. The goal of the stabilization intervention is to hold the top of the tower in place using cables or strips wrapped around the tower. This stabilization procedure is typically employed for provisional interventions (for example to secure post-earthquake structural safety) or when the masonry buttresses need to be removed.

Secondly, the installation of FRP strips requires a very careful approach. The epoxy must be spread evenly and the strip laid as flat as possible or else localized flaws could lead to global failure of the retrofit. This is particularly challenging for applications on masonry structures: old masonry walls are often irregular and rugged. Finally, it should be considered that the long term behavior of FRPs is often unsatisfactory, with high reductions of strength with ageing (Sivaraja et al. 2013; Turk and Cosgun 2012; Marouani et al. 2012). Furthermore, the use of FRPs is often not permitted by statutory conservation bodies on masonry monuments in their portfolio, given the low reversibility and compatibility of FRPs with historic materials. In this situation, structural engineers often opted to use SRGs (Steel Reinforced Grout): these are made of small-diameter (typically 1 mm) high-strength steel cords to form a unidirectional strips to be applied on the surface of masonry

(a)



(b)



**Fig. 3** a Traditional wrapping of a bell tower using steel bars, b application of unidirectional SRG strip

walls using a lime or a low-cement mortar (Fig. 3b) (Razavizadeh et al. 2014; Borri et al. 2015; De Canio et al. 2016).

A technique for the out-of-plane retrofitting has been developed that addresses some of these concerns. Early work by Corradi et al. (2016) suggested that, by using high-strength steel cords embedded in the mortar joints, a reinforced joint repointing could be formed and test results demonstrated that it is possible to increase the masonry shear capacity using this retrofitting method. A similar approach have been recently applied by other researchers (Babaeidarabad et al. 2014; D'Ayala and Paganoni 2014; Wang et al. 2016; D'Antino et al. 2018; D'Ambra et al. 2018; Casacci et al. 2019). The basic idea is to use an inorganic matrix (i.e. a lime or a cement mortar) to bond composite (carbon, glass or basalt fibres) materials to the masonry. This method, known as Textile Reinforced Mortar (TRM), is based on the pioneering experiments of Papanicolaou et al. (2008), which was intended for the analysis of interface debonding and masonry substrate.

The use of metal fasteners or profiles to prevent rocking of wall panels is not new. Steel ties have been used from the 19th century for this purpose in many areas of Europe (Canglia and Barna 1992; Ferreira et al. 2019). Wrapping of masonry domes at the base (abutments) using steel bars is another traditional intervention used to absorb the thrust. Previous research (Ghobarah and El Mandooh 2004; Ceroni et al. 2009; Corradi et al. 2018) then used these metal elements to retrofit small buildings, assembled in the laboratory or tested on site.

Apart from steel rod and FRP wrappings, limited technical solutions are available for the out-of-plane reinforcement of historic masonry buildings. The addition of RC (Reinforced Concrete) ring beams at the eaves level is a questionable retrofitting method, considering the high stiffness and mass of these beams. Damage produced by earthquakes demonstrated the non-effectiveness of this retrofitting method when applied to low-quality masonry (Spence and Coburn 1992; D'Ayala 2004). To overcome these issues, an experimental program recently conducted by Borri et al. (2016) and Sisti et al. (2016) consisted of the use of a composite-reinforced masonry ring beam.

In this area, this paper describes a method for reinforcing masonry buildings against out-of-plane seismic actions. The method consists in the use of steel cables fully embedded into the mortar bed joints and anchored to the walls parallel to the seismic load (i.e. return walls). The used steel cable was made of 7 twisted steel strands of high strength steel. The 7-strand cable had 1 WRC (Wire Rope Center) and six strands wrapped around the central one. Each strand was made of 19 wires. An experimental investigation was carried out in the laboratory and an analytical procedure was used for design purposes. The analytical analysis is general, although it was originally developed for FRP strengthening applied to masonry structures. The main aim is to find a solution to prevent or delay walls' out-of-plane rocking during earthquakes, while complying with the principles of building conservation in terms of minimal (least) intervention (or conservative repair), reversibility and sustainability, as defined by Morris (1877), and ICOMOS charters (Venice Charter 1964; ICOMOS–ISCARSAH Committee 2003).

## 2 Experimental work

### 2.1 Geometry

To investigate the effects of the cable wraps, two full-scale, identical, brickwork specimens were constructed and tested. Each specimen was tested four times: twice without the steel cable reinforcement (undamaged and damaged conditions), and twice, after reinforcement, according to two different loading conditions. Geometries of the masonry specimens and wrap applications are shown in Figs. 4 and 5.

Each masonry specimen consisted of three wall panels to form a C-shaped structure: two wall panels were connected to the strong RC wall of the laboratory. To enhance the understanding of the out-of-plane behavior of actual walls in buildings it's been tried to construct these walls as high as real existing structures. Thickness of the walls was 240 mm (double-whyte), height 2660 mm. The total length of the face-loaded wall was 2430 mm.

It is worth noting that there is no brick interlocking at the intersection between the face-loaded and return walls (Fig. 4): this connection was made only using the same mortar employed for construction, and it created a vertical continuous mortar joint. This was made on purpose to simulate a weak level of wall-to-wall connection, common in historic constructions.

Since the aim of this experiment was to study the wall-to-wall connection and the effect of the cable reinforcement, the in-plane rocking of the return walls was prevented by connecting them to the RC strong wall. The connection between the two return walls and the RC strong wall was secured by 18 steel anchors embedded (for a length of 300 mm) in the wall's mortar bed joints and epoxied in holes drilled in the RC strong wall (Fig. 5). The anchors were uniformly distributed along the height of the return walls (9 anchors/wall). Using an embedment length of 300 mm, preliminary pull-out tests of the steel anchors from brickwork masonry demonstrated a pull-out capacity of 7.6 kN: this was considered sufficient to effectively anchor the return wall to RC strong wall.



**Fig. 4** The two C-shaped brickwork specimens. In the two boxes, it can be noted the vertical mortar joint used to connect the wall panels at the edges [the blue strip was only used during curing time for safety constraints]

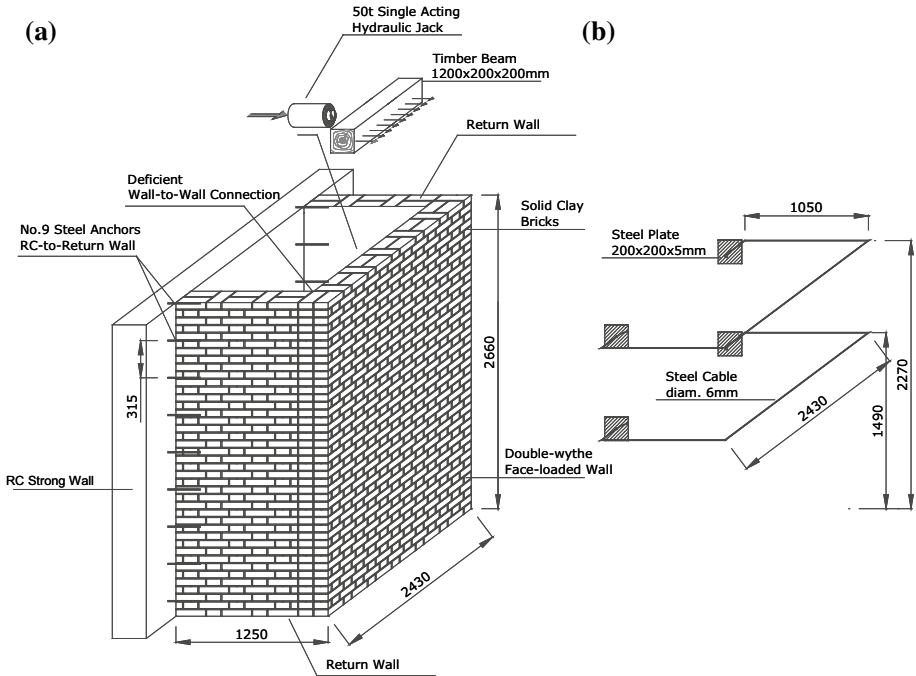


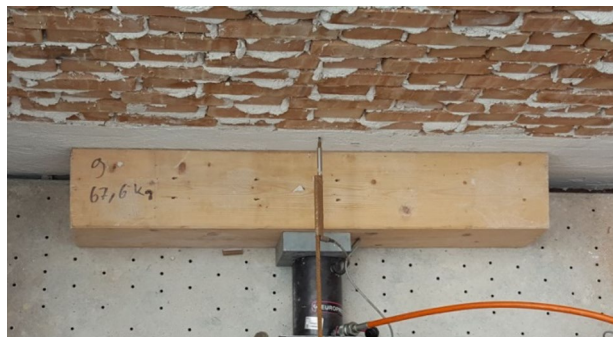
Fig. 5 a The C-shaped masonry specimen, b layout of the wire position (dimensions in mm)

No axial compressive load was applied over the face-loaded wall. It is well established that the effect of axial load on the out-of-plane strength can be significant. However, axial load produces a stabilizing moment on the face-loaded wall, standing against the out-of-plane rocking, and it was decided not to apply it.

## 2.2 Test set up

One hydraulic actuator was placed horizontally inside the C-shaped brickwork structure (Fig. 6). The actuator was used to apply the out-of-plane, monotonic, horizontal load and it was clamped in place at two different heights: (1) to simulate the seismic action [i.e. a

Fig. 6 Detail (horizontal plan) of the position of the out-of-plane load: this was applied using a hydraulic cylinder and distributed using a timber spreader beam



triangular-vertically-distributed horizontal load] at a vertical distance of 1750 mm ( $2/3$  of the panel's height) from the base of the brickwork specimen [i.e. point of application of the equivalent point load] (Loading Configuration No. 1), and (2) in correspondence of the upper reinforcing cable (at a vertical distance of 2270 mm from the base) (Loading Configuration No. 2).

The actuator acted, on a side, on the strong wall and, on the other side, on the face-loaded wall. To distribute the horizontal load, a 1200 mm long spreader timber beam (cross section  $200 \times 200$  mm) was horizontally placed between the actuator and the face-loaded wall, avoiding the development of high stresses near the point of application of the load. In conclusion, the horizontal load was symmetrically applied on the face-loaded wall over a surface of  $200 \times 1200$  mm.

The movements of the face-loaded wall panel were recorded in 6 different locations. The horizontal mid-span deflections were measured using a 100 mm-travel LVDTs (Linear Variable Differential Transducer) with an accuracy of 0.01 mm, at a height of 1950 mm (LVDT1). The wall-to-wall connection was also monitored using 4 LVDTs installed on the face-loaded wall. Finally, relative displacements between wall panels were also recorded at the top (LVDT6). Figure 7 shows the different LVDT positions. For practical and consistency reasons, the LVDTs were positioned outside the C-shaped brickwork specimens.

The load protocol consisted in load cycles: the load limits of each cycle were 3.5, 7, 14 kN. Load was manually applied using a hydraulic pump, connected to the actuator, with

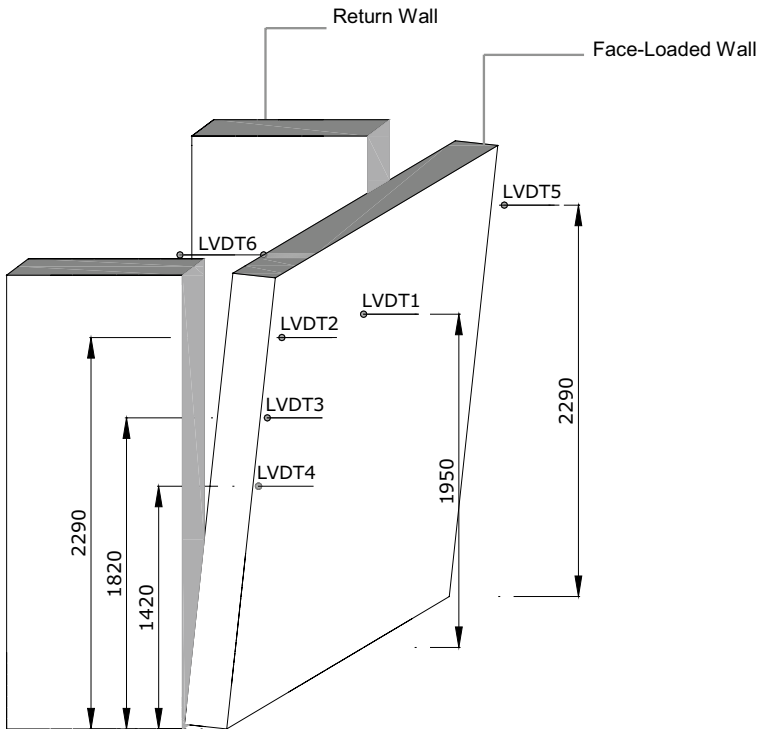


**Fig. 7** Position of LVDTs, measuring horizontal deflections (LVDT1 is located at mid-span) (dimensions in mm)



a gradient of 40–60 N/s. The horizontal load limit was kept acting for a duration of 30 s, and then removed. The brickwork specimens were left unloaded for a duration of further 30 s, before the following load cycle was applied.

### 2.3 Material properties

Five steel cable specimens were cut out of the coil for mechanical characterization. These cables were tested in tension and their strains recorded with a 50 mm gauge length mechanical extensometer. Unfortunately, the strain gauges malfunctioned (most probably because of cable surface resulting in defective bonding of the gauge to the cable surface) and no useful results were obtained from these coupon tests. The average of the five coupon test values is given in Table 1 and is consistent with the manufacturer's minimum value.

Two types of mortar were used in this experiment: mortar No. 1 was a high lime-based product (mix design by weight: 80% sand, 15% lime, 5% Portland cement) and it was used for wall construction, and mortar No. 2 (denomination "Kimisteel MX Calce", manufactured by Kimia ldt), made of a mix of lime and cement (mix design by weight: 64% sand, 28% lime, 6% Portland cement, 2% additives), was employed to repoint the joints where the cables were to be installed. Both types of mortars were ready-to-use products. It was decided to attempt to measure the mechanical properties of the two mortars using a three-point simply supported beam bending test arrangement similar to that used in BS EN 1015-11 (1999). Four three-gang moulds for mortar prisms 40×40×160 mm were used to test in bending (12 tested specimens) and in compression (24 specimens) the two types of mortars (Table 2).

With regard to the bricks, these were clay, durable, high strength, solid engineering bricks, specially manufactured by Toppetti ldt (Masserano, Italy) to cope with exposure to aggressive conditions (product denomination "Mattone Pieno"). Bricks (240×120×55 mm in dimensions) were tested in accordance with EN 771-1 Standard (2011). Test results are also reported in Table 2.

### 2.4 Retrofitting method

The proposed retrofitted method consists in the application of two steel cables embedded into the bed joints of the C-shaped brickwork specimen. The basic idea is to prevent out-of-plane rocking of the face-loaded wall by connecting it to the return walls, using two steel cable wraps. The cables are invisible and fully embedded into the horizontal joints, thus allowing the preservation of the fair-faced aspect of the brickwork masonry.

Two horizontal cuts were made using an electric disc cutter (Fig. 8) to allocate the steel cables into the mortar joints of the outdoor surface of the brickwork specimen.

**Table 1** Properties of the steel cable (ASTM 2002)

Cable diameter (mm)	6
Number of strands/cable	7
Number of wires/strand	19
Yielding load (kN)	21.42 (0.124)
Failure load (kN)	24.58 (0.151)
Yielding strength (MPa)	882.5

CoV coefficient of variation in ( )

**Table 2** Properties of used mortars and bricks

Brick	Compressive strength (MPa)	19.01 (0.121)
	Weight density (kg/m <sup>3</sup> )	1623
	Bending strength (MPa)	3.61 (0.187)
Mortar No. 1 (used for wall construction)	Compressive strength (MPa)	3.58 (0.065)
	Weight density [hardened] (kg/m <sup>3</sup> )	1727
	Bending strength (MPa)	1.09 (0.107)
Mortar No. 2 (used for cable embedment)	Compressive strength (MPa)	17.27 (0.0226)
	Weight density [hardened] (kg/m <sup>3</sup> )	1917
	Bending strength (MPa)	4.16 (0.098)

*CoV* coefficient of variation in (%)

**Fig. 8** The use of an electric disc cutter to make the slots for the steel cables



**Fig. 9** A mastic gun was used before and after the application of the steel cable for joint repointing



Attention was focused on cleaning the joints and removing dust and inconsistent material. Figure 5 shows the wall elevation with the actual dimensions. A mastic gun and a trowel were used to apply the new mortar (Fig. 9) to the prepared cuts, before and after the application of the cables.



**Fig. 10** Detail of a curved metal strip and its application: this was applied at wall edges (in the bed joint) and interposed between the masonry and the steel cable

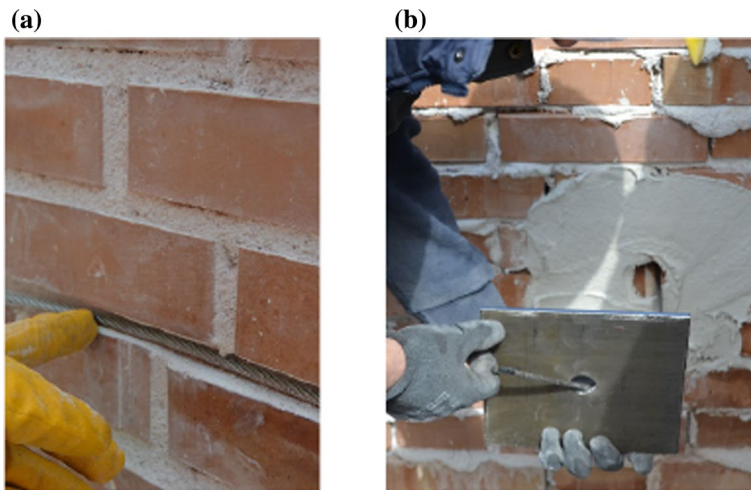


**Fig. 11** **a** Detail of the application of the steel cable inside the bed joint and **b** the used anchoring system on the return walls. The anchoring system is applied inside the C-shape brickwork specimen

In order to prevent local crushing in the masonry near the edges of the walls, small curved metal strips (Fig. 10) were interposed between the masonry and the steel cable. This served to distribute the load transmitted from the cable to the masonry, during loading.

Cables were anchored to the return walls using a steel plate (dimensions  $200 \times 200 \times 5$  mm) and a pre-tensioning device. From the bed joint (Fig. 11a) on the outdoor wall surface, the cable was driven into a hole in the wall and anchored to the steel plate (Fig. 11b) on the indoor surface of the C-shaped brickwork specimen. The steel plate was perforated in the centre: the cable was inserted in the hole and pre-tensioned up to a load of 4 kN (20% of the strap capacity), using a tensioning device (Fig. 12).

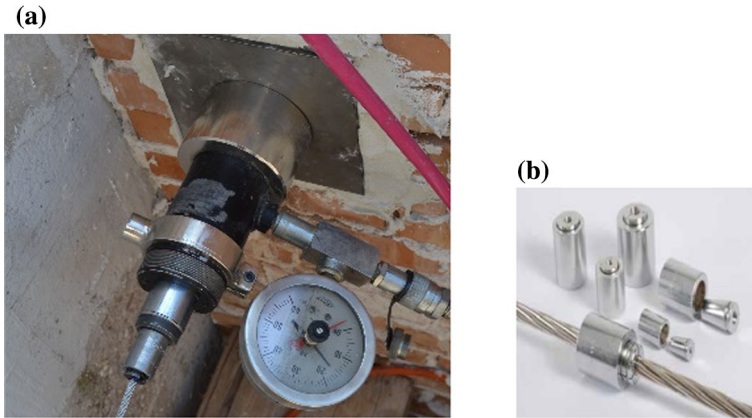


**Fig. 12** The pre-tensioning device consisted in a hollow hydraulic jack used to pull the cable up to a tensile load of 4 kN (a) and a funnel-shaped steel clamp (b)

### 3 Design and analysis

Masonry buildings are often made of natural (stone) and artificial (brick) elements. These structures present specific and diverse stone and brick bond typologies, for which several design approaches have been proposed in the past. For the out-of-plane analysis of masonry buildings, the so-called macro-element method was proposed in the 1970s and became popular in Italy in the 1990s for the calculation and design of the seismic capacity of historic masonry buildings. This method consists in decomposing the masonry building into rigid structural components. For the out-of-plane capacity of single wall panels and entire buildings, the Italian Building Code requires the use of a condition of equilibrium of moments: it basically consists in considering the overturning moments created by inertial forces, activated by the seismic action, and the stabilizing moments, due to vertical forces and anti-seismic devices (ties, wall-to-wall connections, wrappings, etc.) (Italian Building Code 2018; Italian Guidelines 2019).

By using the material laws, and the conditions of structural equilibrium between the masonry macro-elements, it is possible to reduce the degrees of freedom of the structure under investigation, resulting in a more resource- and time-efficient analysis and computation. The reader should be alerted that not all masonry structures can be modeled and studied using the macro-element method: it would be difficult to assess the structural response of very low quality masonry (for example rubble stone masonry) buildings, or multi-leaf stone walls with the macro-element method and caution is recommended. On opposite, it is accepted that solid brickwork masonry structures can be efficiently analyzed with this method.

#### 3.1 Design of the unreinforced specimen

The design of the seismic capacity of a masonry building initially requires to identify the possible collapse mechanisms and then to calculate the corresponding horizontal failure load. For the brickwork C-shaped specimen, there are three possible collapse mechanisms. Figure 13 shows these mechanisms. Out-of-plane rocking is shown in Fig. 13a, while Fig. 13b, c

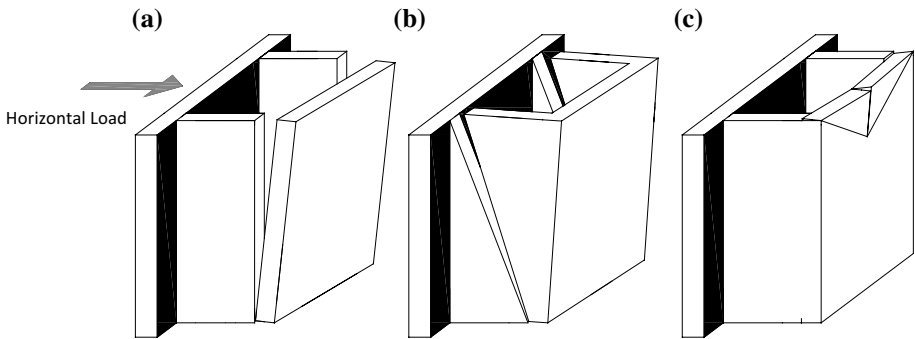


**Fig. 13** **a** Failure due to out-of-plane rocking of the face-loaded wall panel, **b** rocking and shear/bending failure, **c** arch-mechanism

illustrate the out-of-plane mechanism due to shear/bending failure of the return walls and the development of an arch-mechanism, respectively.

In a real case-scenario, a building will collapse when the smallest failure seismic load among all failure loads of all possible mechanisms is achieved. The mechanism in correspondence to this smallest load will be the one effectively observed during an earthquake. Figure 14 show three different out-of-plane mechanisms produced by the seismic action. Clearly, the development of a mechanism depends on several parameters: (1) the mechanical properties of the masonry, (2) the quality level of the wall-to-wall connections, (3) the magnitude of the vertical static loads, (4) the geometry of the building and its wall panels, (5) the position and dimensions of the openings in the walls. In this experiment, only parameter No. 2 was considered. This is clearly a limitation of this experimental work, but it allowed to gain relevant information and data on the effectiveness of the proposed retrofitting method.

As previously noted, the masonry specimens were constructed at the laboratory with a very weak wall-to-wall connection. In this situation, the most likely collapse mechanism of the unreinforced specimens is an out-of-plane rocking of the face-loaded wall. The corresponding failure load  $F_H$ , from the condition of equilibrium of moments, is:

$$W\left(\frac{b}{2}\right) - F_H\left(\frac{2}{3}h\right) = 0 \quad (1)$$



**Fig. 14** Examples of out-of-plane mechanisms: **a** façade's out-of-plane rocking, **b** out-of-plane mechanism and shear/bending failure, **c** arch-mechanism

where  $W$  is the total weight of the face-loaded wall,  $b$  is the thickness (240 mm) of the double-wythe brickwork wall, and  $h$  the height of the C-shaped specimen (2660 mm).  $l$  is the length of the rocking wall panel (2430 mm). The resulting value of  $F_H$  is 1.71 kN. Figure 15 shows the design procedure for a generic 2-story building.

Equation (1) does not take into account the wall-to-wall connection, mainly produced by the mortar-to-brick bonding and the brick-to-brick interlocking at the base of the wall panel. Figure 16 illustrates this.

Similarly to the design procedure used for retaining walls in cohesive soils, where cohesion has a positive effect in preventing overturning, the design procedure given by Eq. (1) can be re-formulated to include the mortar-to-brick bonding at the intersection between return and face-loaded walls (Fig. 17).

Assuming a linear and elastic relationship between stress and strain for the mortar in tension, a revised out-of-plane failure load  $F_H$  can be re-calculated:

$$W\left(\frac{b}{2}\right) - F_H\left(\frac{2}{3}h\right) + \sigma_m \times 2b \times h_m\left(h - \frac{h_m}{3}\right) = 0 \tag{2}$$

where  $h_m$  is:

$$h_m = \frac{\left(\frac{2F_H}{h} - \sigma_m \times 2b\right)h^2}{2F_H} \tag{3}$$

and  $\sigma_m$  is the mortar-to-brick bonding strength, equal to 0.05 MPa. The value of  $\sigma_m$  has been experimentally calculated: standardized pull-out tests (BS EN 1542 1999) were initially carried out in the laboratory to estimate the mortar adhesion (Fig. 18). A average mortar tensile strength 0.31 MPa was found. Brick-to-mortar bond was also measured according to the test layout shown in Fig. 19: after removing the contribution of the

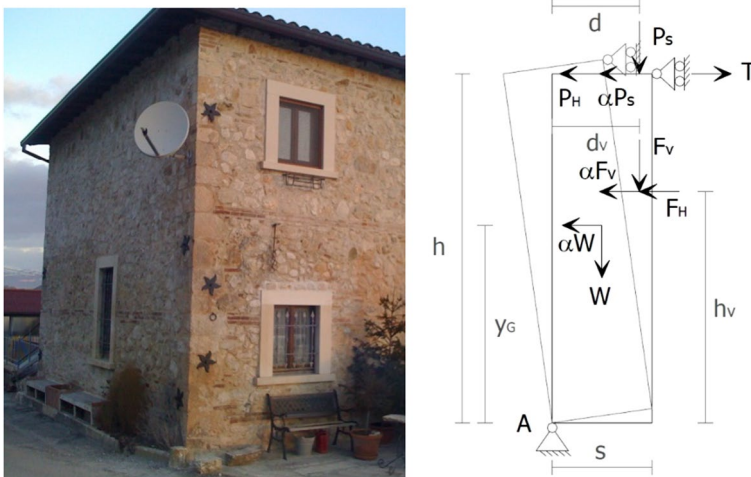


**Fig. 15** General procedure for the calculation of the rocking coefficient  $\alpha$  of a 2-story building, using the condition of equilibrium of moments about point A [ $W$  = weight of the façade,  $F_V$  = vertical load of the first floor,  $F_H$  = thrust (in case of vaulted or arch-structures),  $T$  = reaction of a tie (if any),  $P_S$  = weight of the roof structure,  $P_H$  = thrust of the roof structure (if any)]

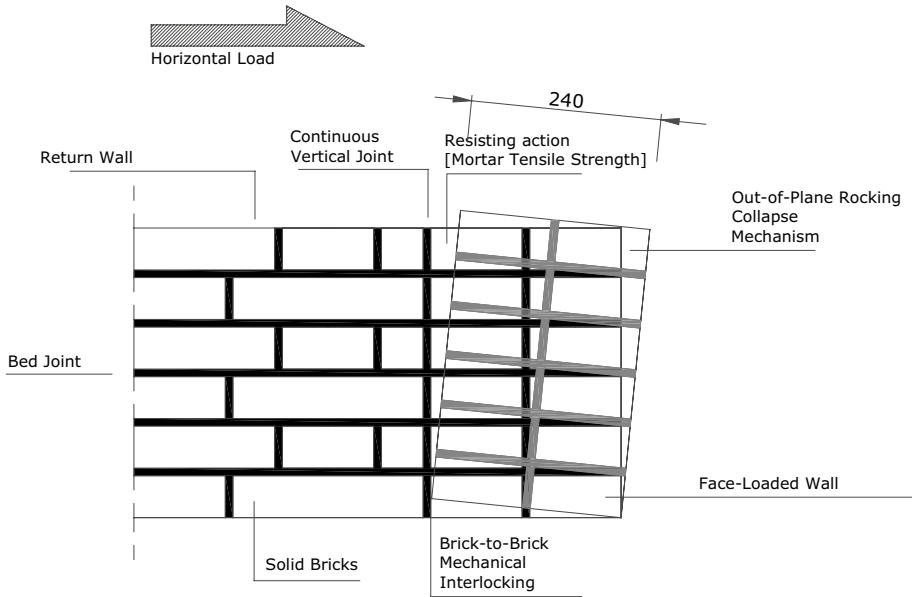


Fig. 16 Detail of the rocking mechanism at the base of the brickwork specimen (dimensions in mm)

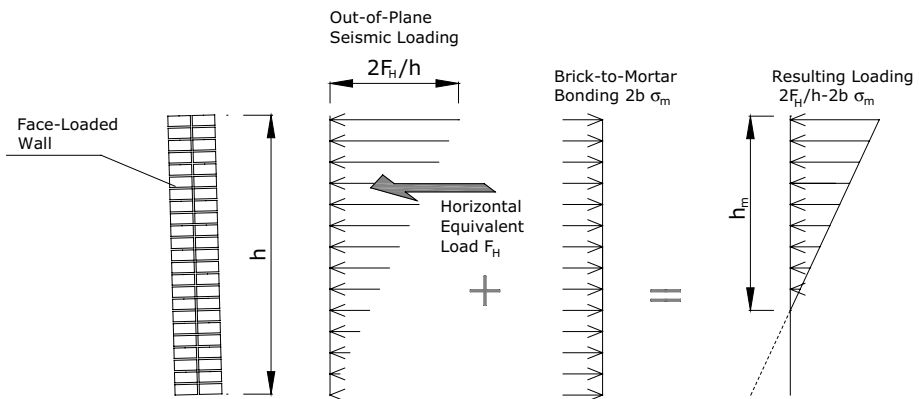
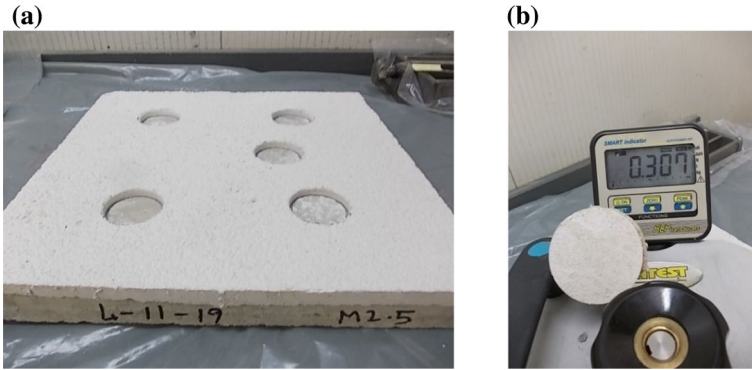
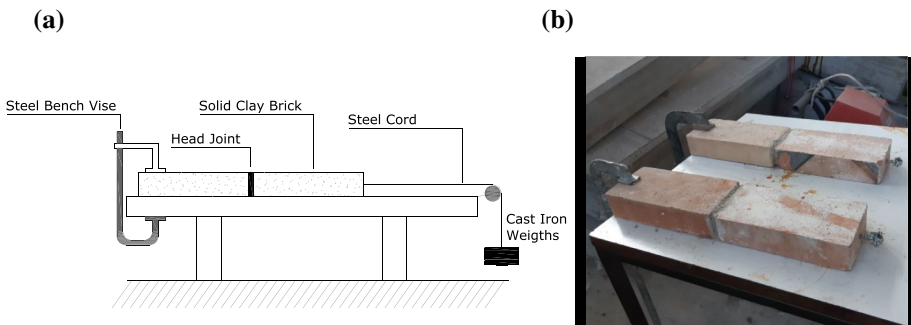


Fig. 17 Horizontal loads applied on the faced-loaded wall

friction, an average bond strength of 0.0563 MPa was found from these tests. Standard deviation was 0.0127 MPa. Once the values of  $\sigma_m$  and  $h_m$  have been computed, it is possible to re-calculate  $F_H$ . This is now much higher (38.68 kN) compared to the previous value (1.71 kN), denoting a critical contribution of the mortar.



**Fig. 18** Mortar tensile strength (pull-out tests): **a** Mortar No. 1 was laid over a concrete slab; **b** detail of the pull-out instrument



**Fig. 19** Brick-to-mortar bond tests: **a** test layout, **b** brickwork specimens

### 3.2 Design of the reinforced specimen

Brickwork specimens have been re-tested after reinforcement. The mortar-to-brick bonding at the wall-to-wall connection is now equal to zero (as a consequence of the development of a vertical crack at mortar-to brick interface, during tests on unreinforced specimens).

For design purposes, we can assume that the load-capacity of the face-loaded wall is governed by the strength of the steel cables. In this situation, the resisting action is now provided by the steel cable and the weight of the rocking wall panel. These produce a stabilizing moment about the base of the brickwork specimen:

$$W\left(\frac{b}{2}\right) - F_H\left(\frac{2}{3}h\right) + T_2 \times h_w = 0 \tag{4}$$

where  $T_2$  is the yielding load of the upper steel cable (21.42 kN) and  $h_w$  is the vertical distance between the panel's base and the upper cable (2270 mm). Only the contribution upper cable was considered in Eq. (4). Two loading configurations were used (Fig. 5): for both of the them, the calculated value of  $F_H$  is very high (29.62 and 23.14 kN for loading configuration No. 1 and No. 2, respectively), and different collapse mechanisms should be considered.



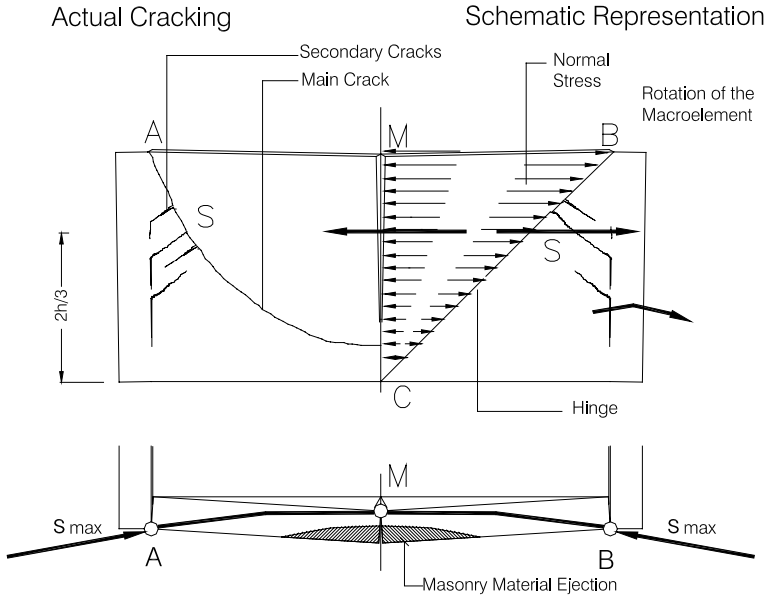


Fig. 20 Arc mechanism

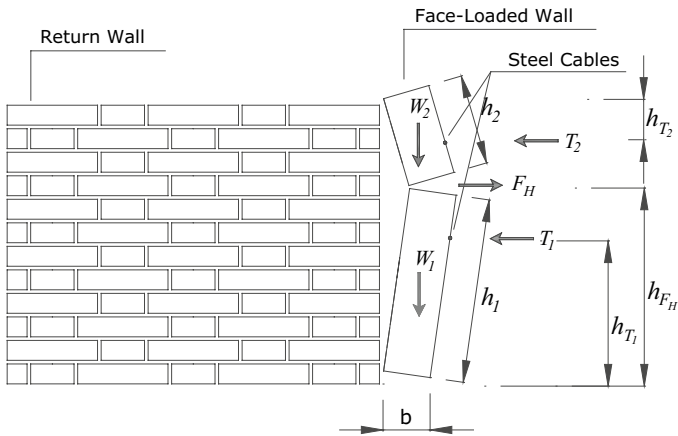


Fig. 21 Vertical bending mechanism

If we consider the failure modes shown in Figs. 20 and 21 (vertical and horizontal bending), the load-capacity of the face-loaded wall needs to be re-calculated. Figure 20 shows a schematic representation of the well-known “arc-mechanism” (or horizontal bending): the failure of the face-loaded wall occurs when three aligned vertical cylindrical hinges simultaneously develop. However the hinge at point M (Fig. 20) cannot “open” due to the presence of the steel cable. This mechanism could develop only if we assume that phenomena of slippage of the steel cable in the bed joint could occur.

Figure 21 shows another collapse mechanism (vertical bending). This mechanism is likely to occur when the loading configuration No. 1 is used. The load-capacity of the face-loaded wall can be calculated with:

$$W_1\left(\frac{b}{2}\right) + W_2b + \frac{h_1}{h_2}\left[\left(W_2\frac{b}{2}\right) + T_2h_{T_2}\right] + T_1h_{T_1} - F_Hh_{F_H} = 0 \tag{5}$$

where  $T_2$  is the yielding load of the upper steel cable (21.42 kN), and  $h_{T1}$ ,  $h_{T2}$ ,  $h_{FH}$ ,  $h_1$  and  $h_2$  are given in Fig. 21. Using Eq. (5), the load-capacity  $F_H$  of the face-loaded wall is 57.51 kN

### 4 Test results

Each brickwork specimen was tested four times: two tests were carried out with the specimen in an unreinforced configuration to measure its structural response before and after cracking. Two further tests were conducted after reinforcement.

#### 4.1 Unreinforced specimens

Experimental capacity values of unreinforced specimens can be seen in Table 3 to be greater than values predicted by the condition of equilibrium of moments, considering the equilibrium of the brickwork wall subjected to the out-of-plane loads. Equation (1) drastically under-predicts the out-of-plane capacity by 82% and 102%, with the largest degree of error occurring for the specimen No. 2. The equilibrium Eq. (1) under-predicts the experimental results because it does not account for the contribution of the mortar in the wall-to-wall connection. These results suggest that the equilibrium equation provides a minimum value of the out-of-plane capacity, but it is not able to capture the specimen actual behavior.

**Table 3** Test results

	Maximum out-of-plane load (kN)	Failure mode	Corresponding horizontal movement* (mm)	Residual load (kN)
URM_1	11.63	Face-loaded wall rocking	0.669	3.85
URM_2	10.17	Face-loaded wall rocking	0.403	4.24
(mean)	(10.90)			(4.04)
RMA_1	4.03	Face-loaded wall rocking	8.43	3.91
RMA_2	4.38	Face-loaded wall rocking	7.88	4.11
(mean)	(4.21)			
RFC_M_1	13.77	Arc-mechanism	8.07	13.61
RFC_M_2	17.13	Arc-mechanism	9.32	15.73
(mean)	(15.45)			(14.47)
RFC_S_1	11.67	Macro-element rocking	10.48	10.40
RFC_S_2	13.27	Shear failure	3.63	7.73
(mean)	(12.47)			(9.05)

\*LVDTI

**Fig. 22** Horizontal load vs. mid-span horizontal deflection (LVTD1) (face-loaded wall) (Specimen No. 1)

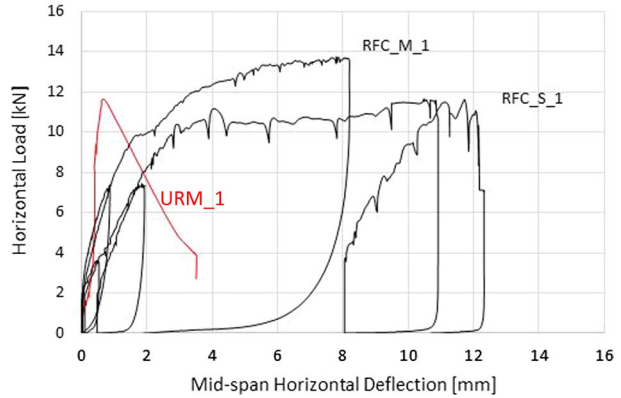
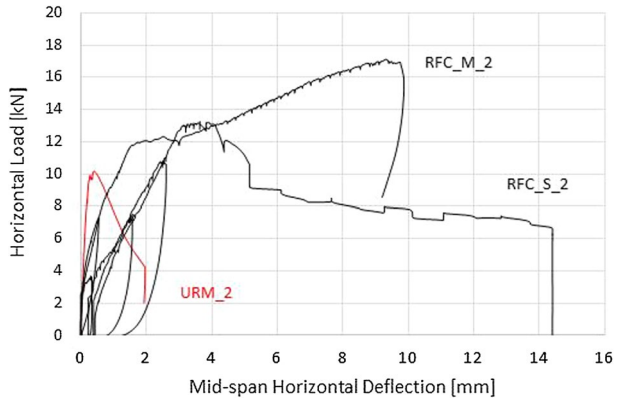


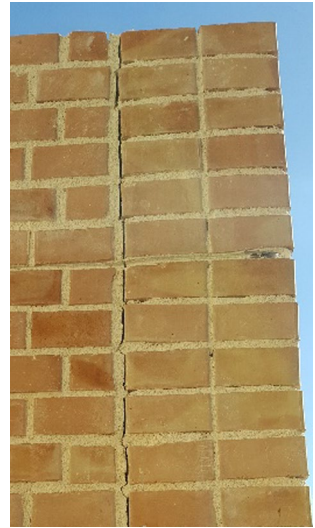
**Fig. 23** Horizontal load vs. mid-span horizontal deflection (LVTD1) (face-loaded wall) (Specimen No. 2)



Two series of tests were carried out on the URM specimens: URM-series refers to undamaged (control) specimens, while RMA-series to damaged specimens. It can be noted that the overall out-of-plane average capacity is very different for the two series (Figs. 22 and 23): this was 10.9 and 4.21 kN for the URM- and RMA-series respectively. The failure mode of the URM-series consisted in the development of a vertical crack (Fig. 24) along the mortar joints at the wall-to-wall connection (connection between return and face-loaded wall). A residual capacity of 4.04 kN was also recorded after cracking, with a reduction of 63% compared to the magnitude of the maximum applied load.

Brickwork specimens were subsequently re-tested to assess the contribution of the mortar by comparison with previous results (RMA-series). The horizontal load, producing the activation of rocking mechanism, drastically reduced (from 10.9 to 4.21 kN), as a consequence of the missing contribution of the bonded wall-to-wall connection. When the maximum load was reached, the load remained almost constant with increasing horizontal movements (zero-stiffness). It is worth noting that no load drop was recorded after the maximum load capacity was reached. Furthermore, the calculated rocking load (1.71 kN) is now more similar to the one recorded in the experiments (4.21 kN). The difference can be caused by the unaccounted friction and interlocking resistance along the cracked surface.

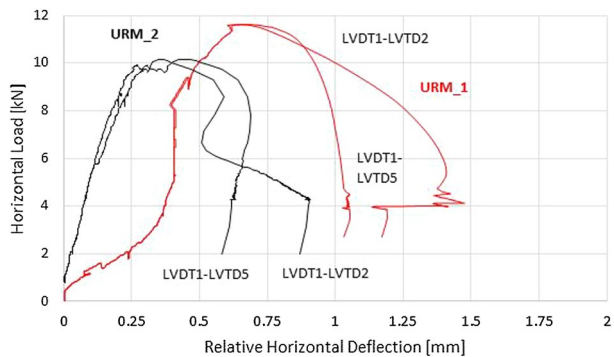
**Fig. 24** Out-of-plane rocking mechanism of unreinforced specimen



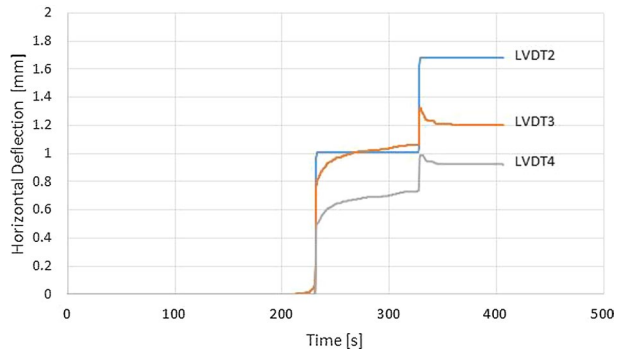
The bending (out-of-plane) deformations of the face-loaded wall panel can be studied by comparing the horizontal deflections measured using the LVDTs at different points. Bending deformations are linked to the relative horizontal displacements (LVTD1–LVTD2 and LVTD1–LVTD5), where LVTD1 is located near the point of application of the hydraulic cylinder at the mid-span of the face-loaded wall (Fig. 7). These were very small for URM specimens (0.62 and 0.35 mm at maximum load for URM\_1 and URM\_2 respectively) (Fig. 25), and almost negligible for RMA ones. Figure 25 also shows that the magnitudes of the horizontal movements (LVDT2 and LVDT5) at the ends of the face-loaded wall are very similar.

Figure 26 shows the horizontal movements vs time of LVDT2, LVDT3 and LVDT4 (Fig. 7). It can be noted that the ratios between the vertical distance of each LVTD from the panel’s base and the horizontal movement were sufficiently constant, and the resulting curvature on the horizontal plane was very small. This indicated that a flexural failure (or arc-mechanism) was avoided and was part of the reason that such a large horizontal displacement was measured for LVTD1. Therefore, the collapse mechanism of the face-loaded wall panel was due to a rigid rotation (out-of-plane rocking) about the hinge at its base.

**Fig. 25** Relative horizontal movements at 2/3 of the panel height (URM-series, final loading cycle). The small magnitude of the relative movements demonstrates the limited bending deformation of the wall panel perpendicular to the direction of the horizontal load



**Fig. 26** URM2 test: horizontal movements of the three LVDTs located at 2290 mm (LVDT2), 1820 mm (LVDT3) and 1420 mm (LVDT4) above the base of the brickwork specimen. Horizontal movements decrease moving from the panel's top to the bottom (rocking mechanism)



Although a flexural failure was not produced both the capacity and displacement validated that the method of analysis using masonry macro-elements can be effective in the assessment of the seismic capacity of masonry buildings. The use of equilibrium equations can provide a minimum value of the out-of-plane capacity, and it is able to capture the specimen actual behavior. Consequently, it may be concluded that the boundary (wall-to-wall connection) conditions of the walls subjected to out-of-plane loads are critical for the assessment of the out-of-plane capacity of the wall panels of a building. This is a very well-known conclusion, in agreement with the outcomes of several another studies and post-earthquake buildings' survey by the authors involving walls subjected to out-of-plane actions but, unexpectedly, tests results have shown that a low-quality mortar joint can highly contribute to overall capacity of the brickwork specimens.

## 4.2 Reinforced specimens

A total of four tests were carried out on the reinforced brickwork structures (each specimen was tested twice, using the two loading configurations). The effectiveness of the cable reinforcement can be effectively assessed by comparing the overall capacity of reinforced specimens with the one of unreinforced. However, for unreinforced specimens, we may use test results for URM or RMA series, and a preliminary discussion is needed: the main difference is that, for URM specimens, the capacity is partially governed by the wall-to-wall bond, given by the mortar used to connect the face-loaded wall to the return walls. On opposite, for damaged walls (RMA series), the capacity mainly depends on the stabilizing moment given by the weight of the face-loaded wall. For both damaged (RMA series) and reinforced walls (RFC\_M and RFC\_S series) the contribution of the wall-to-wall bond is negligible (these walls are all damaged, i.e. return walls separated from face-loaded wall), and, by comparing the capacity of RMA specimens with the one of reinforced, it is possible to better assess the contribution of the cable reinforcement. In a real case scenario, when this intervention is carried out on undamaged structures, it is clear that the wall-to-wall connections can play a critical role, reducing the positive effect of the cable reinforcement.

The reinforced structures, shown in Figs. 5 and 6, performed well under the cyclic horizontal load. These resisted approximately 227 and 196% more load (for loading configuration No. 1 and 2, respectively) compared to the same structures in unreinforced cracked configuration (RMA specimens). Table 3 shows the test results: it can be noted that the mean out-of-plane capacity increased from 4.21 kN (unreinforced, cracked specimens, RMA series) to 15.45 kN and 12.47 kN for loading configuration No.1

(RFC\_M series) and 2 (RFC\_S series), respectively (Table 3). The increment of the capacity of the reinforced walls reduced to 41.7% (RFC\_M series) and 14.4% (RFC\_S series), when we compare these results with the ones of URM specimens (undamaged).

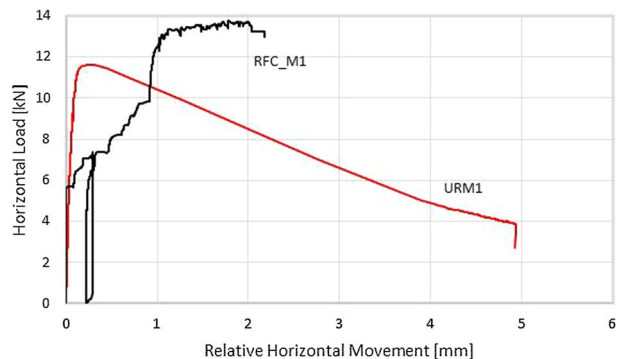
Apart from considerations about the improved out-of-plane capacity, other observations can be drawn. The failure mode changed: the out-of-plane rocking mode was prevented by the application of steel cables. This was the primary objective of this experiment. The steel cables and the anchor system were able to prevent the relative detachment of the face-loaded wall from the return walls, restoring the so-called box-like behavior of the masonry structure, and enabling a beneficial transfer of the horizontal load to the return walls. Figure 27 shows this for an unreinforced and reinforced specimen. It can be noted the reduced magnitude of the relative horizontal movement recorded for the reinforced specimen (FRC\_M1).

Furthermore, it is worth noting that tensile failures of the cables or local ruptures of the anchor system did not occur. Other critical observations can be made about the curved metal strips: these were functional in preventing local failures (shear failure of the steel cables or mortar crushing) at the edges. It can be noted that the pre-tensioning load, applied to the cables during their installation, was able to limit an initial relative detachment of the wall panels, allowing to make cables instantly functional when the out-of-plane load was applied.

The mid-span horizontal displacement (LVDT1) accompanying that maximum load was 8.69 mm and 7.05 mm for RFC\_M and RFC\_S specimens, respectively. Surprisingly, for reinforced specimens, the stiffness of the brickwork structures, given by the slope in the elastic, initial, loading phase of the horizontal load versus LVDT1 curve did not significantly increase. This can be attributed to the fact that the cable reinforcement was applied to damaged specimens (RMA series). On the contrary, a higher stiffness can be noted for unreinforced URM specimens, as a consequence of the action of the brick-to-mortar bonding contribution at walls intersection. The application of the steel cable reinforcement increased the horizontal load-capacity of the structures without reducing their deformation-capacity. This is the consequence of several concurrent causes: the high deformation capacity of the steel cables, phenomena of slippage at mortar-to-cable interface, small mechanical adjustments of the retrofitting system.

However, the steel cable reinforcement was not able to prevent other local collapse mechanisms, reducing the increment of the load-capacity after reinforcement. A secondary aim of this research was to prevent local collapse mechanisms, using the steel

**Fig. 27** Relative movements of face-loaded and return walls for unreinforced (URM1) and reinforced (RFC\_M1 specimens)



reinforcement, and to convert the face-loaded wall into a laterally-constrained plate, reinforced, on the tension side, with the steel cables.

The face-loaded walls exhibited three different modes of failure: (1) arc-mechanism due to the opening of three vertically-aligned cylindrical hinges (two wall macro-elements); (2) out-of-plane rocking of a portion of the face-loaded wall; (3) shear failure.

#### 4.2.1 Arc-mechanism

This was the most frequent mode of failure and it consisted in the development of three horizontal and cylindrical hinges on the face-loaded wall: one at the base, one near the point of application of the horizontal load and another at the top of face-loaded wall (Fig. 28a). This failure mode occurred for both structures of the RFC\_M series. The three hinges divided the face-loaded wall in two masonry macro-elements. With the increasing horizontal movement of the face-loaded wall, two further cylindrical hinges developed near the steel cables (Fig. 28b). A cracking noise during the test revealed a progressive cracking of the mortar near the area where the hinges appeared. Phenomena of deboning of the steel cable from the embedding mortar were not recorded. It is worth noting that the arc-type failure mode is clearly governed by the method of application of the load (this is basically a concentrated load). Since seismic loads are inertial and, thus, distributed, it can be concluded the used method of load application was not able to properly simulate the seismic action. However, we believe that the application of a concentrated load was also particularly challenging for the out-of-plane stability of the face-loaded wall itself. The recorded value of out-of-plane capacity of the wall can be regarded as a lower bound value of its capacity under a seismic action.

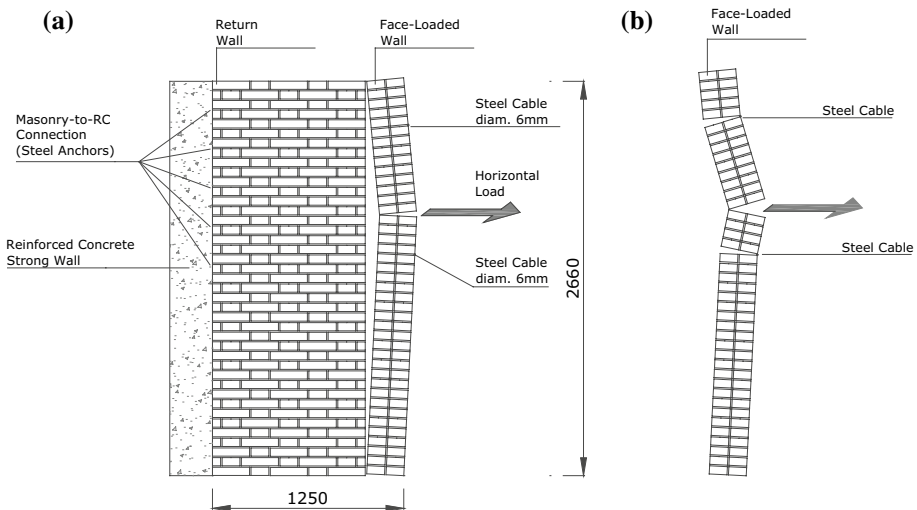


**Fig. 28** Failure mode of RFC\_M series: **a** the 3-hinge mechanism initially developed, **b** by increasing the horizontal load this became a 5-hinge mechanism

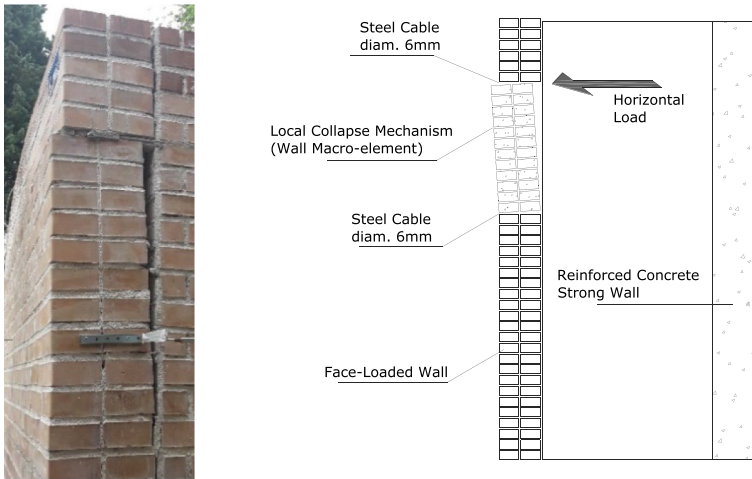


Fig. 29 Out-of-plane mechanism of a reinforced specimen (RFC\_S\_1)

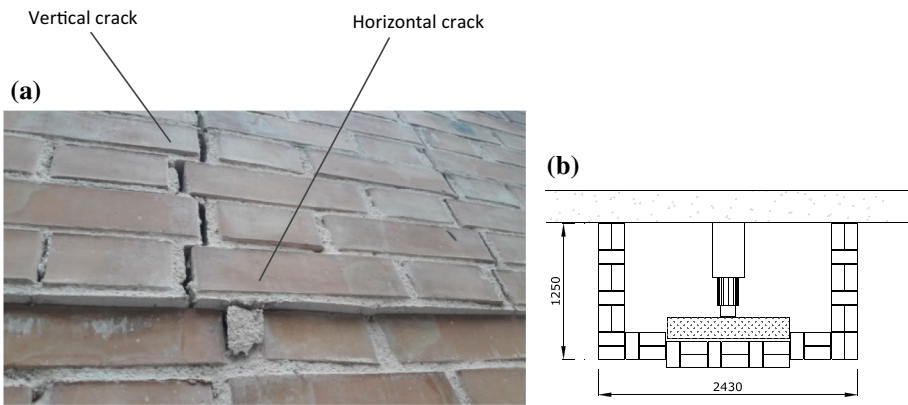


Fig. 30 Shear mechanism of a reinforced specimen (RFC\_S\_2): **a** detail, **b** schematic representation [plan view] (dimensions in mm)

#### 4.2.2 Out-of-plane rocking

The second recorded failure mode consisted in the development of a single cylindrical hinge at the level of the lower steel cable wrapping (Fig. 29). This failure mode occurred for test No. RFC\_S\_1. The horizontal load was applied at the same level of the upper steel cable wrapping (Loading Configuration No.2): this caused the out-of-plane rocking of the masonry macro-element confined between the two steel cable wrappings. This macro-element rotated, at the base, about the hinge and slid with scarcely any noise, at the top, along the mortar bed joint.



### 4.2.3 Shear failure

The third failure mode was only observed for test No. RFC\_S\_2. This consisted in the horizontal expulsion of a portion of brickwork masonry confined between the two steel cables. Sliding phenomena (horizontal cracking) were recorded along the bed joints, where the cables were installed, and in the head joints (vertical zig-zag cracking). Figure 30 shows the failure mode: it is evident that the length and position of the wooden beam used to distribute the load had an influence on the failure mode. However, the maximum capacity of the face-loaded wall was recorded before vertical cracking occurred, and this reduced the effect of the length of the wooden beam: the failure mode initially consisted in the sliding phenomena (horizontal cracking).

The corresponding horizontal-load capacities (maximum load) of the three failure modes described above were not very different. Load capacities of reinforced structures ranged between 11.67 and 17.13 kN: this scattering can be considered normal for a non-homogenous, non-isotropic material, made with limited controls during the construction phase.

Starting from the load-capacity of the unreinforced cracked specimens (4.21 kN), it can be concluded that the steel-cable reinforcement is able to significantly increase the overall structural capacity, but, once the out-of-plane rocking of the face-loaded wall is prevented by the application of the reinforcement, it is complicated to identify the failure mode of the reinforced structures. Several failure modes are possible: tiny variations in the method of application of the load, geometry of the walls, defects in construction may result in the development of a particular crack pattern as opposed to another one. This implies that we cannot likely improve the horizontal-load capacity further: once we prevent the activation of a failure mode, another one will immediately develop.

## 5 Conclusions

This initial attempt to validate the effectiveness of a new retrofitting method using high strength steel cables demonstrates that it is possible to increase the building capacity to resist out-of-plane actions. Compared to the more traditional steel cable or rod wrapping of historic buildings, the main innovation of this experiment consists in the embedment of the steel cables directly into the mortar bed joints, thus preserving the fair-faced aspect of the brickwork masonry. This required the use of small diameter steel cables (6 mm). Interesting is also the use of an anchorage system of the steel cable to the return walls: this consisted in a mechanical device able not only to anchor the cable, but also to pre-stress it making it immediately functional.

Given accurate information on material property evolution and walls' geometry, two full-scale brickwork assemblages have been tested in the laboratory under controlled conditions. The aim was to simulate the action of the seismic action, using a horizontal line-load applied at the top of the brickwork specimens.

A total of 8 out-of-plane tests have been conducted. The primary result from the experiments is the enhancement in the out-of-plane capacity of the reinforced specimens, from 4.21 kN (unreinforced specimens, RMA-series) to 15.45 kN (reinforced specimens, RFC\_M-series), respectively.

Two different positions of the horizontal load have been used to test the reinforced specimens (RFC\_M series and RFC\_S series). Test results demonstrated that, by switching the

vertical position of the horizontal out-of-plane load, different collapse mechanisms developed, while the out-of-plane capacity remained basically unchanged. In both cases, the steel cables were able to prevent the relative detachment of the face-loaded from the return walls. The out-of-plane rocking of the face-loaded wall was effectively avoided.

This paper also considered a design procedure for both unreinforced and reinforced structures. However, the out-of-plane capacity of the unreinforced brickwork specimens was not consistent with the analytical one, calculated using the macro-element method. The very different out-of-plane capacities of un-damaged (URM-series) and damaged (RMA-series) unreinforced specimens denoted the critical contribution of the wall-to-wall connection. In this area, a better understanding of the boundary conditions is believed to be fundamental for the assessment of the out-of-plane capacity of a masonry building. A similar result was obtained for the reinforced structures: none of the used design procedures was able to capture the experimental out-of-plane capacity of the reinforced specimens.

As we continue the experimental investigation, we wish to develop further examples and isolate those details that are critical to making accurate design predictions. We believe that a limitation of this experimental work is the applied concentrated line-load, used to test the walls, given the inertial and dynamic characteristics (thus resulting in a more distributed horizontal load) of the seismic loading. Within new tests, we wish to learn more about the failure modes and phenomena of progressive damage of both unreinforced and retrofitted brickwork specimens.

**Acknowledgements** The authors would like to acknowledge the support of the Reluis Consortium through grant number “Linea Murature 2018–2019”. Our thanks are also extended to Kimia Ltd. (Perugia, Italy—supplier of the steel cable reinforcement and special mortars used for joint repointing). The authors also thank Alessio Molinari and Emanuele Bombardieri, and the technical staff of the Structures Laboratory (Lastru) of the University of Perugia, Italy.

**Authors’ contribution** MC co-wrote the first draft of the paper with ES, contributed to the design and analysis of both the unreinforced and reinforced specimens, and to the interpretation of the experimental results. GB contributed to the design and analysis of out-of-plane response, supervised the construction phase of the brickwork specimens, participated in joint analysis and contributed to paper writing. All authors read and approved the final manuscript.

**Funding** The authors acknowledge the support of the Reluis Consortium through grant number “Linea Murature” and Kimia Inc. (Perugia, Italy).

**Availability of data and material** The datasets are available from the corresponding author on reasonable request.

## Compliance with ethical standards

**Conflict of interest** The authors Corradi and Speranzini declare no conflict of interest. Mr Bisciotti, master student at the University of Perugia, worked at Kimia, but this had no influence on the experimental work and analysis.

**Open Access** This article is licensed under a Creative Commons Attribution 4.0 International License, which permits use, sharing, adaptation, distribution and reproduction in any medium or format, as long as you give appropriate credit to the original author(s) and the source, provide a link to the Creative Commons licence, and indicate if changes were made. The images or other third party material in this article are included in the article’s Creative Commons licence, unless indicated otherwise in a credit line to the material. If material is not included in the article’s Creative Commons licence and your intended use is not permitted by statutory regulation or exceeds the permitted use, you will need to obtain permission directly from the copyright holder. To view a copy of this licence, visit <http://creativecommons.org/licenses/by/4.0/>.

## References

- ASTM D2256 (2002) Standard test method for tensile properties of yarns by the single-strand method
- Babaëdarabad S, Loreto G, Arboleda D, Nanni A (2014) FRCM-strengthened CMU masonry walls subjected to out-of-plane load. *Mason Soc J* 32(1):69–84
- Borri A, Corradi M (2019) Architectural heritage: a discussion on conservation and safety. *Heritage* 2(1):631–647
- Borri A, Castori G, Corradi M, Speranzini E (2015) Durability analysis for FRP and SRG composites in civil applications. *Key Eng Mater* 624:421–428
- Borri A, Corradi M, Sisti R, Giannantoni A (2016) Experimental analysis of masonry ring beams reinforced with composite materials. In: *Proceedings 16th international brick and block masonry conference*. Padua, Italy, 26–30 June 2016
- BS EN 1015-11 (1999) Methods of test for mortar for masonry. Determination of flexural and compressive strength of hardened mortar
- BS EN 1542 (1999) Products and systems for the protection and repair of concrete structures. Test methods. Measurement of bond strength by pull-off
- BS EN 771-1 (2011) Specification for masonry units. Clay masonry units
- Bui TT, Limam A, Sarhosis V, Hjiad M (2017) Discrete element modelling of the in-plane and out-of-plane behaviour of dry-joint masonry wall constructions. *Eng Struct* 136:277–294
- Caniglia S, Barna GL (1992) *Handbook of industrial refractories technology: principles, types, properties and applications*. William Andrew, Norwich
- Casacci S, Gentilini C, Di Tommaso A, Oliveira DV (2019) Shear strengthening of masonry wallets resorting to structural repointing and FRCM composites. *Constr Build Mater* 206:19–34
- Ceroni F, Pecce M, Manfredi G (2009) Seismic assessment of the bell tower of Santa Maria del Carmine: problems and solutions. *J Earthq Eng* 14(1):30–56
- Corradi M, Borri A, Castori G, Sisti R (2016) The reticulatus method for shear strengthening of fair-faced masonry. *Bull Earthq Eng* 14(12):3547–3571
- Corradi M, Di Schino A, Borri A, Rufini R (2018) A review of the use of stainless steel for masonry repair and reinforcement. *Constr Build Mater* 181:335–346
- D’Ambra C, Lignola GP, Prota A, Sacco E, Fabbrocino F (2018) Experimental performance of FRCM retrofit on out-of-plane behaviour of clay brick walls. *Compos B Eng* 148:198–206
- D’Antino T, Carozzi FG, Colombi P, Poggi C (2018) Out-of-plane maximum resisting bending moment of masonry walls strengthened with FRCM composites. *Compos Struct* 202:881–896
- D’Ayala D (2004) Unreinforced brick masonry construction. EERI, *World Housing Encyclopedia*
- D’Ayala DF (2014) Conservation principles and performance based strengthening of heritage buildings in post-event reconstruction. In: Ansal A (ed) *Perspectives on European earthquake engineering and seismology*, vol 34. Springer, Dordrecht, pp 489–514
- D’Ayala DF, Paganoni S (2011) Assessment and analysis of damage in L’Aquila historic city centre after 6th April 2009. *Bull Earthq Eng* 9:81–104
- D’Ayala DF, Paganoni S (2014) Testing and design protocol of dissipative devices for out-of-plane damage. *Proc Inst Civil Eng Struct Build* 167:26–40
- D’Ayala D, Speranza E (2003) Definition of collapse mechanisms and seismic vulnerability of historic masonry buildings. *Earthq Spectra* 19(3):479–509
- De Canio G, de Felice G, De Santis S, Giocoli A, Mongelli M, Paolacci F, Roselli I (2016) Passive 3D motion optical data in shaking table tests of a SRG-reinforced masonry wall. *Earthq Struct* 40(1):53–71
- de la Llera JC, Vásquez J, Chopra AK, Almazán JL (2000) A macro-element model for inelastic building analysis. *Earthq Eng Struct Dyn* 29(12):1725–1757
- Di Nino S, Luongo A (2019) A simple homogenized orthotropic model for in-plane analysis of regular masonry walls. *Int J Solids Struct* 167:156–169
- Ferreira TM, Mendes N, Silva R (2019) Reducing the seismic vulnerability of existing buildings: assessment and retrofit. *Buildings* 9(6):148
- Ghobarah A, El Mandooh Galal K (2004) Out-of-plane strengthening of unreinforced masonry walls with openings. *J Compos Constr* 8(4):298–305
- Gilstrap JM, Dolan CW (1998) Out-of-plane bending of FRP-reinforced masonry walls. *Compos Sci Technol* 58(8):1277–1284
- Giresini L, Pantò B, Caddemi S, Calì I (2019) Out-of-plane seismic response of masonry façades using discrete macro-element and rigid block models. In: *7th ECCOMAS thematic conference on computational methods in structural dynamics and earthquake engineering (COMPdyn 2019)*. Crete Island, Greece

- Guidelines to Italian Building Code (2019), Istruzioni per l'applicazione dell'«Aggiornamento delle «Norme tecniche per le costruzioni»» di cui al decreto ministeriale 17 gennaio 2018. Rome, Italy (**in Italian**)
- Hamed E, Rabinovitch O (2005) Out-of-plane bending of URM walls strengthened with FRP strips—modeling and analysis. In: Proceedings of the 7th international symposium on fiber reinforced polymer (FRP) reinforcement for concrete structures, Kansas City, MO, November 6–9, 2005, pp 249–68
- Hamed E, Rabinovitch O (2007) Out-of-plane behavior of unreinforced masonry walls strengthened with FRP strips. *Compos Sci Technol* 67:489–500
- ICOMOS–ISCARSAH Committee (2003) ICOMOS charter—principles for the analysis, conservation and structural restoration of architectural heritage. In: Proceedings of the ICOMOS 14th general assembly and scientific symposium. Victoria Falls, Zimbabwe, vol 2731
- Italian Building Code (2018) Aggiornamento delle Norme tecniche per le Costruzioni—NTC 2018. Rome, Italy (**in Italian**)
- Italian Senate, Report No. 01077470 (2017) Earthquakes. Central Italy 2016, Emilia 2012, L'Aquila 2009: reconstruction resources and laws. Rome, Italy
- Jurina L (2017) Cerchiatura e messa in sicurezza provvisoria di edifici storici: alcuni esempi, Ingenio-web. <https://www.ingenio-web.it/7014-cerchiatura-e-messa-in-sicurezza-provvisoria-di-edifici-storici-alcuni-esempi>
- King R (2015) The industrial geography of Italy. Routledge, Abingdon
- Korany Y, Drysdale R (2006) Rehabilitation of masonry walls using unobtrusive FRP techniques for enhanced out-of-plane seismic resistance. *J Compos Constr* 10(3):213–222
- Lagomarsino S, Resemini S (2009) The assessment of damage limitation state in the seismic analysis of monumental buildings. *Earthq Spectra* 25(2):323–346
- Marouani S, Curtil L, Hamelin P (2012) Ageing of carbon/epoxy and carbon/vinylester composites used in the reinforcement and/or the repair of civil engineering structures. *Compos B Eng* 43(4):2020–2030
- Milani G, Lourenço P, Tralli A (2006) Homogenization approach for the limit analysis of out-of-plane loaded masonry walls. *J Struct Eng* 132(10):1650–1663
- Modena C, Valluzzi MR, Tongini Folli R, Binda L (2002) Design choices and intervention techniques for repairing and strengthening of the Monza cathedral bell-tower. *Constr Build Mater* 16:385–395
- Morris W (1877) The SPAB manifesto. Society for Protection of Ancient Building (SPAB), London
- Paganoni S, D'Ayala D (2014) Testing and design procedure for corner connections of masonry heritage buildings strengthened by metallic grouted anchors. *Eng Struct* 70:278–293
- Papanicolaou CG, Triantafyllou TC, Papathanasiou M, Karlos K (2008) Textile reinforced mortar (TRM) versus FRP as strengthening material of URM walls: out-of-plane cyclic loading. *Mater Struct* 41(1):143–157
- Putrino V, D'Ayala D (2020) Effectiveness of seismic strengthening to repeated earthquakes in historic urban contexts Norcia 2016. *Disaster Prev Manag* 29(1):47–64
- Razavizadeh A, Ghiassi B, Oliveira DV (2014) Bond behavior of SRG-strengthened masonry units: testing and numerical modeling. *Constr Build Mater* 64:387–397
- Sisti R, Corradi M, Borri A (2016) An experimental study on the influence of composite materials used to reinforce masonry ring beams. *Constr Build Mater* 122:231–241
- Sivaraja SS, Thandavamoorthy TS, Vijayakumar S, Aranganathan SM, Dasarathy AK (2013) Preservation of historical monumental structures using fibre reinforced polymer (FRP)-case studies. *Procedia Eng* 54:472–479
- Spence R, Coburn A (1992) Strengthening buildings of stone masonry to resist earthquakes. In: Calladine CR (ed) *Masonry construction*. Springer, Dordrecht, pp 213–221
- Tumialan JG, Galati N, Nanni A (2003) Fiber-reinforced polymer strengthening of unreinforced masonry walls subjected to out-of-plane loads. *ACI Struct J* 100(3):321–329
- Turk AM, Cosgun C (2012) Seismic behaviour and retrofit of historic masonry minaret. *Gradevinar* 64(1):39–45
- Velazquez-Dimas JI, Ehsani MR (2000) Modeling out-of-plane behavior of URM walls retrofitted with fiber composites. *J Compos Constr* 4(4):172–181
- Venice Charter (1964) International charter for the conservation and restoration of monuments and sites, (ICOMOS). In: Proceedings of the 2nd international congress of architects and technicians on historical monuments. Venice, Italy
- Wang C, Forth JP, Nikitas N, Sarhosis V (2016) Retrofitting of masonry walls by using a mortar joint technique; experiments and numerical validation. *Eng Struct* 117:58–70
- Wang C, Sarhosis V, Nikitas N (2018) Strengthening/retrofitting techniques on unreinforced masonry structure/element subjected to seismic loads: a literature review. *Open Constr Build Technol J* 12:251–268

**Publisher's Note** Springer Nature remains neutral with regard to jurisdictional claims in published maps and institutional affiliations.